Thermal evolution of vibrational properties of α-U

J. Bouchet and F. Bottin
CEA, DAM, DIF, 91297 Arpajon Cedex, France
(Received 19 August 2015; published 11 November 2015)

By means of *ab initio* molecular dynamics calculations, the thermal evolution of vibrational properties in α-U is studied at low temperature. The phase transition undergone by this material around 50 K was previously studied extensively using *ab initio* calculations in the framework of the linear response at 0 K. Although these previous efforts capture successfully the complexity of the experimental phonon spectrum at room temperature, in particular the soft-phonon mode and its pressure dependence, they fail to reproduce the transition to the charge-density-wave state at ambient pressure as a function of temperature. In the present work, by going beyond the quasiharmonic approximation and taking into account the temperature effects explicitly, we are able to reproduce the behavior of both phonon spectrum and elastic constants of U-α as a function of temperature.

DOI: 10.1103/PhysRevB.92.174108 PACS number(s): 63.20.dk, 62.20.de

I. INTRODUCTION

Density functional theory (DFT) has been an extraordinary successful tool to understand the ground state properties of the actinides [1–5] and to show the fundamental role played by the 5f electrons [6]. The inclusion of temperature effects in the calculations is even more challenging but crucial for studying the rich phase diagram exhibited by these elements.

Usually, thermal vibrations of atoms can be taken into account via the so-called quasiharmonic approximation (QHA). In this framework, the phonon dispersion relations are calculated at 0 K using density functional perturbation theory [7] (DFPT) and the temperature is included only via the thermal dilatation, i.e., by computing the phonon spectrum at different volumes. This method has been applied with success to Th [8]. However with only one f electron and a fcc structure, Th does not show all the complexity found in the heavier actinides. In particular, this method cannot be used on structures stabilized at high temperature by anharmonic effects and therefore dynamically unstable at 0 K such as the bcc structure adopted by the whole actinide series before the melting point [9,10].

Uranium stands as one of the most intriguing materials, exhibiting as it does many puzzling properties [11]. Among pure metals, uranium is the only one to adopt the α-U structure in its ground state (other metals present such orthorhombic symmetry under pressure, such as Pr and Pa); see Fig. 1. To date, it is also the only element in the periodic table in which a charge-density-wave (CDW) state is observed at room pressure. The origin of the three phase transitions observed in uranium at low temperature remained a mystery for almost two decades. One crucial experiment was carried out by Crummett *et al.* [12] in 1979, using neutron inelastic scattering to determine the phonon dispersion curves. They revealed a spectacular softening of one phonon branch (named Σ_4) with a soft mode situated almost in the middle of the [100] direction [12]. The decisive experiment was carried out a year later when Smith *et al.* [13] monitored the behavior of this branch with temperature. For this mode, frequency steeply declines with temperature, down to zero, which is typical of a soft-mode transition. Smith *et al.* [13] concluded that a doubling of the unit cell occurs along the x direction, together with a lattice distortion, due to the presence of a CDW. This new structure, α_1, is shown in Fig. 1. Subsequent to the three CDW transitions (one for each direction), the approximate volume of the unit cell is 6000 Å^3, 300 times the volume of the α cell.

Using DFPT, Bouchet [14] was able to reproduce the neutron-scattering data obtained 30 years ago. What is immediately apparent is the good agreement between experiment and theory, the most remarkable result certainly being that obtained for the [100] direction, for which the complexity of the spectrum is clearly reproduced. In particular, the softening observed in the Σ_4 mode is quite well described by DFPT. Pressure strongly influences the CDW transitions in uranium and therefore the softening of the Σ_4 branch. Bouchet [14] predicted an increase of the energy of the soft phonon, a prediction confirmed 3 years later by inelastic x-ray scattering [15]. More recently, the QHA was applied at different volumes, and was not able to reproduce the whole complexity of the phonon dispersion curve [16]. The failure of this approximation was due to the soft mode behavior in temperature, which cannot be reproduced by its pressure dependency. In fact, experimentally, the volume increases with temperature and the energy of the soft mode goes up, stabilizing the α phase. But in the DFPT calculations, performed at 0 K, the energy of the soft mode rather decreases and becomes imaginary with a slight increase of the volume predicting a dynamical instability of the α phase [14,16].

To overcome this inherent difficulty of the QHA, the temperature has to be directly included in the calculations. For this purpose, a recent approach named SCAILD has been proposed [17] and applied to a large number of metals, in particular the high-temperature bcc phase of uranium [9] which is not stable at 0 K. However, this method seems to overcorrect the temperature effects on the phonon dispersion curve. In the present paper, these effects are included by means of *ab initio* molecular dynamics (AIMD) and the temperature-dependent effective potential technique (TDEP) recently developed by Hellman and coworkers [18,19]. We show that we correctly reproduce the soft mode behavior in temperature and that we observe the α-α_1 phase transition at 50 K. The temperature behavior of the bulk modulus is also well reproduced.

II. SIMULATION METHOD

Simulations were performed using the ABINIT package [20,21] in the framework of the projector augmented wave

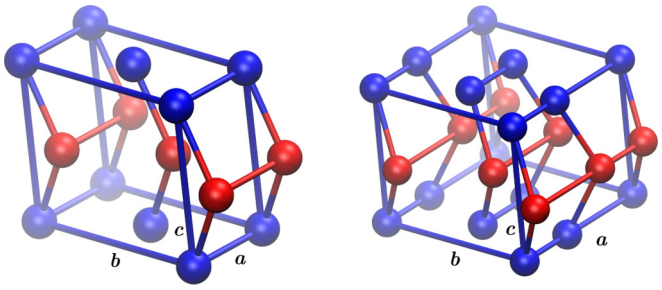

FIG. 1. (Color online) Left: orthorhombic structure of the α phase of uranium. Right: α_1 phase of uranium. The α structure is doubled in the a direction and the blue and red atoms have been slightly displaced in opposite direction corresponding to a charge density wave with $q_x = 1/2$ and $\phi = 90^\circ$.

(PAW) method [22,23] and by means of the generalized gradient approximation (GGA) according to the parametrization of Perdew, Burke, and Ernzerhof (PBE) for the exchange-correlation energy and potential [24]. A better description of electronic correlations (LDA+U, DMFT, ...) is not required for α-U, either at the ground state level [25] or at the level of lattice dynamics [26].

The spin-orbit coupling is not considered in this work since it is known to have negligible effects on uranium equation of state [4,14,27]. Using ATOMPAW [28–30], we generated PAW atomic data with a radius r_{PAW} equals to 1.51 Å, with $6s$, $6p$, $7s$, and $5f$ states as valence electrons.

The cutoff energy chosen for the plane wave set along the AIMD simulations is equal to 435 eV. The α-U structure is modeled using the experimental parameters given by Lloyd and Barrett [31–33] and LeBihan *et al.* [34]. A $4 \times 2 \times 3$ α-U supercell including 96 atoms is used to capture the doubling of the unit cell along the a axis responsible for the appearance of the CDW. Since a large number of **k** points is essential to obtain converged vibrational frequencies, we used a $2 \times 4 \times 2$ Monkhorst-Pack mesh leading to the inclusion of 8 special **k** points in these AIMD calculations. Simulations were performed in the NVT ensemble (constant number of particles, constant volume and temperature). AIMD simulations were run for about 8 ps using a time step (τ) of 2.5 fs. Taking benefit of an efficient scheme of parallelization [35] and using hundreds to thousands of processors, the recovery time is a few months.

The effects of zero-point motion are not included in simulations, since they are expected to be minor for such heavy materials. However, one of the temperature used in this work is lower (50 K) than the Debye temperature of uranium [36] (around 300 K). Consequently, simulations including nuclear quantum effects (such as PIMD, path integral molecular dynamics) would be very useful to verify this assumption.

To extract the vibrational frequencies from the AIMD simulations we used the temperature-dependent effective potential (TDEP) technique developed by Hellman and coworkers [18,19]. In this method, a model Hamiltonian expanded in the harmonic form is used to fit the Born-Oppenheimer molecular dynamics potential energy surface at finite temperature:

$$H = U_0 + \sum_i \frac{\mathbf{p}_i^2}{2m_i} + \frac{1}{2}\sum_{ij} \mathbf{u}_i \Phi_{ij} \mathbf{u}_j, \tag{1}$$

where U_0 is the ground state energy, $\mathbf{p}_i$ the momentum, $\mathbf{u}_i$ the displacement of atom i with respect to equilibrium, and Φ_{ij} the matrix of the interatomic force constants (IFC). In this form, the IFC matrix gives at each AIMD time step τ the forces $\mathbf{F}_i(\tau)$ as a function of the atomic displacements:

$$\mathbf{F}_i(\tau) = \sum_j \Phi_{ij} \mathbf{u}_j(\tau). \tag{2}$$

The AIMD providing a set of forces and displacements, by computing the Moore-Penrose pseudoinverse $u_j^\dagger(\tau)$ of $u_j(\tau)$, the previous equation can be reversed and the IFC matrix [19] evaluated. This TDEP technique amounts to carrying out a least-squares method leading to the best fit of the IFC.

Depending on the system, this matrix can be huge. For the present study, the supercell involves 96 atoms, so 82 944 coefficients have to be potentially calculated. Fortunately, several constraints can be used to drastically reduce this number [19], such as the atomic sum rule, the equivalence of IFC within a shell of nearest neighbors (NN) and the symmetries of the Bravais lattice. Therefore, in the case of this system with a $Cmcm$ structure, by including all the atoms up to the 12th shell of NN in the calculation of the IFC, the total number of coefficients can be reduced to 53. Once the IFC are obtained, a Fourier transform is performed to get the dynamical matrix at any **q** point of the Brillouin zone. We have implemented this method in the ABINIT program and have used a large number of functionalities available in this package. We emphasize that our code takes advantage of all the symmetries found at the level of the unit cell.

III. RESULTS AND DISCUSSION

Three AIMD trajectories at 50, 300, and 900 K have been performed. For simulations at 300 and 50 K, the average atomic positions of the last 2000 time steps, projected in the xy and yz planes, are presented in Fig. 2. In the yz plane we observe no difference between these two temperatures. The average atomic positions correspond perfectly to the ideal positions of the α structure. The situation is different in the xy plane. At 300 K the average positions correspond to the α structure whereas at 50 K the atoms deviate from their ideal positions in the [100] direction. The same pattern is reproduced in the whole supercell, with the two α-U atoms slightly displaced in opposite directions. It is clear that at 50 K, the α-U primitive cell can no longer be used to fill the space. A larger primitive cell, doubled in the x direction, is needed (see the blue box in Fig. 2).

Several remarks can be made. First, we stress that the atomic displacements highlighted above are exactly the ones involved in the phase transition between α-U and α_1-U. It is also interesting to mention that the atomic displacements preserve the C-face centering as proposed by Raymond *et al.* [15]. Such charge-density wave (CDW) is thus represented by sine waves with phase angles of $\pi/4$ and $-\pi/4$ in Fig. 2. Finally, we point out that the magnitude of the lattice distortion u is

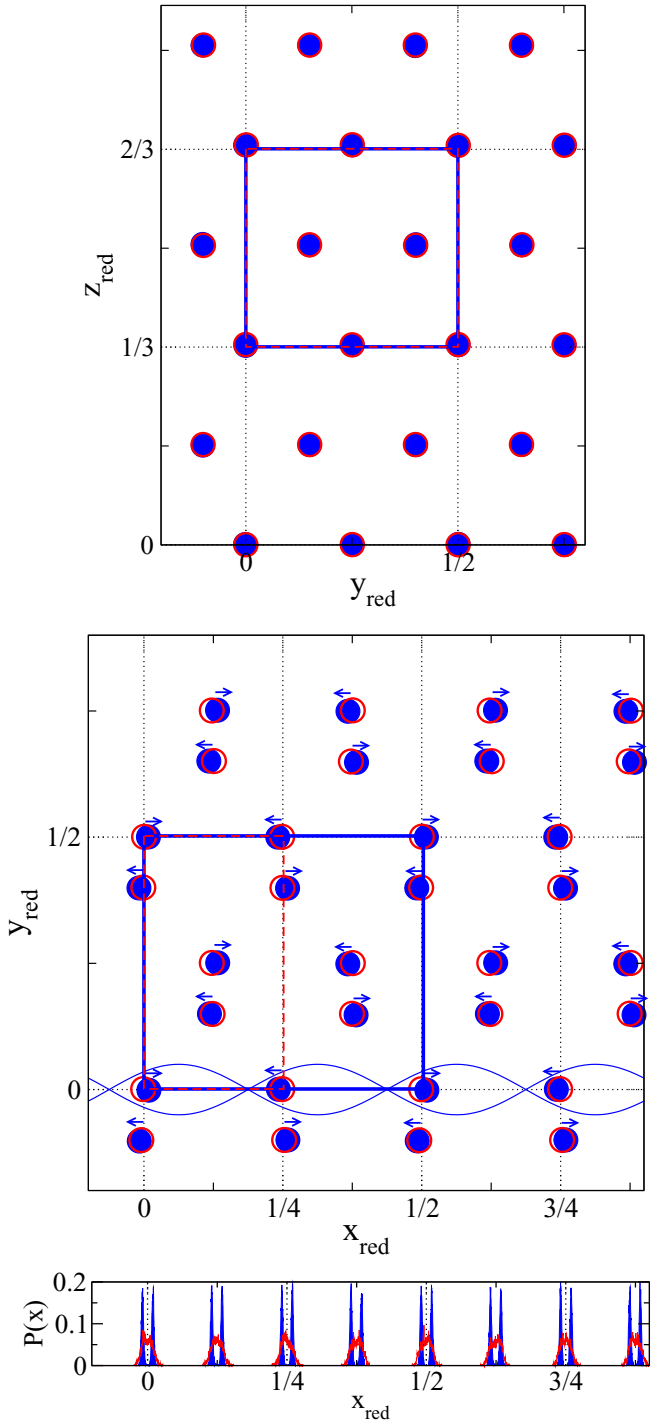

FIG. 2. (Color online) Average atomic positions for AIMD simulations of α-U at 300 K (in open red) and at 50 K (in full blue). The red box (dashed line) indicates the primite α-U cell and the blue box indicates the α_1-U cell. The sinusoidal modulations of the two α-U atoms are represented by the blue lines. At the bottom, $P(x)$ describes the distribution of atomic positions along x.

around 0.2 Å, a value larger that the experimental value of 0.1 Å reported by Nelson *et al.* [37] using extended x-ray absorption fine structure spectroscopy (EXAFS) or the value of 0.03 Å reported by Marmeggi *et al.* [11,38]. This can be due to the limited size of the present supercell and the absence

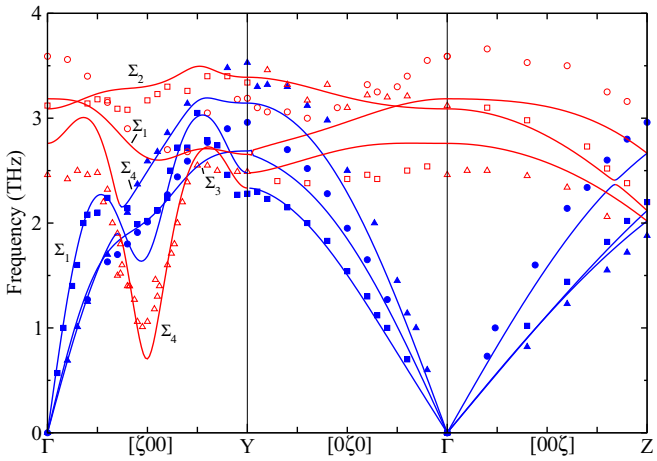

FIG. 3. (Color online) Calculated phonon dispersion curves of α-U at 300 K. Blue lines represent modes which appear to be primarily acousticlike while red lines represent modes which are mostly opticlike. Experimental neutron-scattering data [12] at room temperature are denoted by open and filled symbols.

of strain compared to a real sample or to the choice of the volume since the lattice distortion strongly varies with the lattice parameters [39].

The phonon spectra at 300 K extracted from the corresponding AIMD simulations are presented in Fig. 3 and compared to the experimental neutron-scattering data of Crummett [12] at room temperature. The TDEP spectrum is very close to both the DFPT one [14] obtained at 0 K using the theoretical equilibrium volume and the experimentally measured phonon dispersion. In particular, the extreme complexity of the phonon spectrum is well reproduced with a pronounced dip for the Σ_4 branch and a minimum located near $\mathbf{q} = 1/2$ in the [100] direction [40]. In Fig. 4 we focus on the temperature behavior of the Σ_4 and Σ_1 branches obtained with AIMD at 50, 300, and 900 K. We show also the results of calculations performed using DFPT at 0 K, but with the cell parameters used in the AIMD simulations. As the temperature is lowered from 900 to 50 K the Σ_4 opticlike mode softens in AIMD, with a strong decrease from 0.7 to 0.1 THz between 300 and 50 K. This remarkable result, combined with the change of average atomic positions (see Fig. 2), directly associates the phase transition with the softening of the Σ_4 branch. Furthermore, this also confirms the experiment of Smith *et al.* which observed a large decrease of the frequency of the Σ_4 branch as the temperature is lowered (from 1.01 THz at 300 K to 0 THz around 70 K [11]; see the upper panels of Fig. 4). In DFPT, where we only take into account the volume changes, the Σ_4 mode has a completely opposite behavior. The Σ_4 mode softens with the volume increase, which means that in the QHA the α-U structure is destabilized at room and higher temperature in contradiction with the experimental observations. In AIMD, the softening of the Σ_1 mode is only slightly affected by the temperature while in DFPT it is strongly dependant of the volume changes, with imaginary frequencies at 900 K as observed for Σ_4 (see the lower panels of Fig. 4). This demonstrates the failure of the QHA for uranium and the

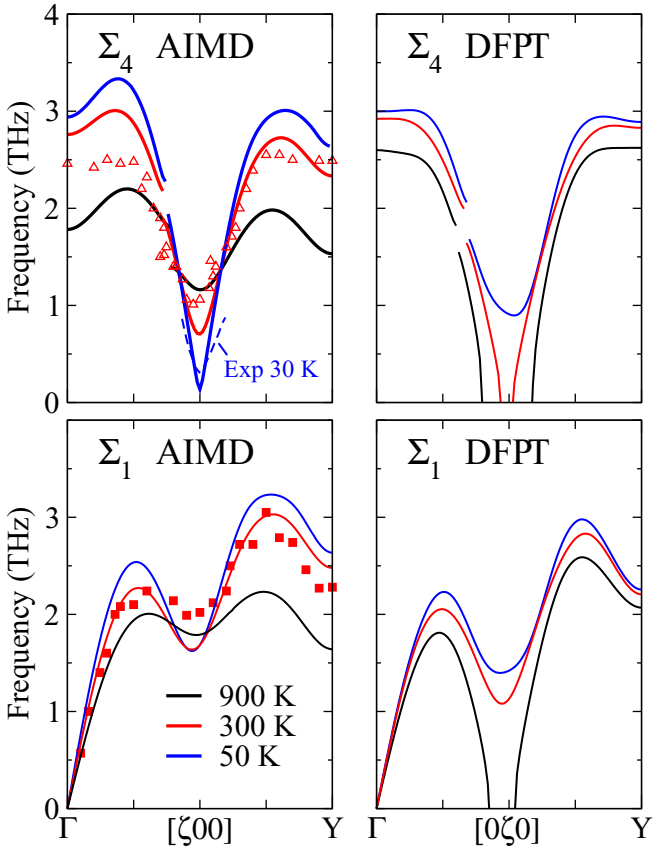

FIG. 4. (Color online) Left: AIMD results at 50 (in blue), 300 (in red), and 900 K (in black) for the Σ_4 and Σ_1 mode of α-U. Experimental neutron-scattering data [12] at room temperature are denoted by open and filled symbols and by the dashed line at 30 K [13]. Right: DFPT calculations with the cell parameters used in the AIMD simulations at 50, 300, and 900 K.

need to include directly the temperature in the calculations to describe the thermal vibrations.

At 900 K, a temperature close to the phase transition towards the β bct structure (941 K) and the γ bcc structure (1048 K), we did not find any anomalies in the phonon spectra, except for those observed at lower temperatures but less pronounced. Therefore it is possible that these phase transitions are not driven by the softening of a phonon mode but more likely by larger phonon entropy of the high-temperature phases. To clarify this question it is necessary to compute the phonon spectra of β and γ phases.

Up to now, phonon spectra were extracted from AIMD simulations using the ideal α-U structure (2 atoms in the unit cell, no distortion $u = 0$ Å). At 50 K, as previously shown, this structure is no longer the most stable and the α_1-U structure (4 atoms in the unit cell, distortion $u \approx 0.2$ Å) becomes the one adopted by uranium. Consequently, we extracted the phonon spectra using 4 atoms rather than 2 in the unit cell and taking into account the distortion u (see in Fig. 5 the long-wavelength part of the dispersion curves along the [100] direction). The minimum of the longitudinal optical (LO) mode Σ_4 (located at Γ when using 4 atoms in the unit cell) strongly increases from 0.1 to 0.8 THz when going from ideal α-U to real α_1-U

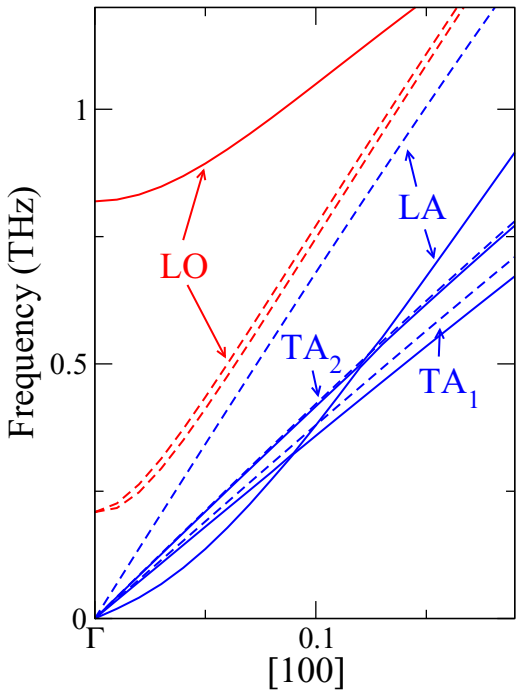

FIG. 5. (Color online) Low-frequency part of the α_1-U phonon spectra for $u = 0.2$ Å (in red and blue solid lines). The dashed lines are the phonon branches of the α-U structure ($u = 0$ Å).

structures. In parallel, the slope of the longitudinal acoustic mode decreases by 40% while the transverse mode are almost unchanged.

By using the relationships between the slope of the acoustic branches and the elastic constants, we are able to compute C_{11}, related to the longitudinal acoustic branch along the x direction. It is well established [42,44] that the elastic moduli of uranium show large anomalies at low temperature, the largest effect being observed in the C_{11} modulus which decreases by a factor of two on cooling from 50 K to 43 K, before increasing between 43 K and 4.2 K. We give in Table I our results for the 3 longitudinal elastic constants of uranium at 300 K and at 50 K, using α-U or α_1-U structures, and compare them to experimental values [41,43] and DFPT [16]. For α-U, at 300 K, present values are close to the ones obtained using DFPT [16] at 0 K and compare reasonably well with the experimental values except for C_{11} which is overestimated by 30% in the calculations. Between 300 K and 50 K the elastic

TABLE I. Elastic constants (GPa) of α-U. The values for α-U at 50 K are in italics since our calculations show that the material is in the α_1 structure at this temperature.

	C_{11}	C_{22}	C_{33}	K
α-U (300 K, this work)	287	177	211	129
α-U (DFPT [16])	259	197	297	129
Exp. (300 K, Ref. [41])	215	199	267	115
α-U (50 K, this work)	*293*	*197*	*258*	*129*
Exp. (50 K, Ref. [42])	174	209	288	113
α_1-U (50 K, this work)	184	184	247	109
Exp. (4.2 K, Ref. [43])	114	211	286	107

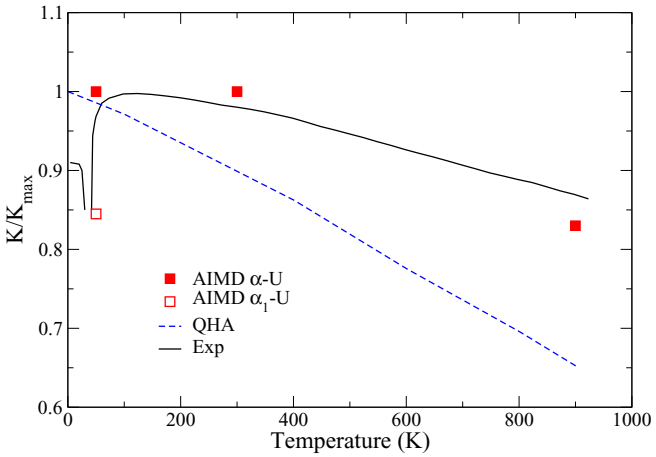

FIG. 6. (Color online) Relative variation of the α-U bulk modulus (with respect to its maximum) as a function of the temperature. The black line is the ultrasound data [43,45]. The red filled and open squares are the AIMD results for both ideal α-U and α_1-U, respectively, and the blue dashed line is the results from QHA [16].

constants for α-U slightly increase while experimentally C_{11} decreases. When rather considering the α_1-U structure, C_{22} and C_{33} remain almost equal but C_{11} strongly decreases by 40% as experimentally observed at the phase transition; see Table I. The bulk modulus K which is a combination of the elastic constants follows the same trend.

Finally we compare our results for the bulk modulus K with the experimental data [43,45] and the QHA results [16]. Figure 6 shows the relative behavior of K with temperature. Whereas the bulk modulus decreases monotonically in QHA, the one obtained using explicit temperature effects clearly reproduces the anomaly at the phase transition around 50 K, due to the softening of the longitudinal acoustic branch from α to α_1. Above 50 K, TDEP results follow the experimental continuous decrease of the bulk modulus with increasing temperature, around 10%–15% between 300 and 900 K, whereas the QHA predicts a larger decrease, around 35%.

IV. CONCLUSIONS

We have shown that the phonon softening of the Σ_4 optical mode in α-U can be reproduced correctly by extracting the phonon spectra from AIMD simulations following the method proposed by Hellman and coworkers [18]. Whereas all previous attempts based on the QHA failed to reproduce the behavior of this mode as a function of temperature, this one can capture the effects responsible for the CDW phase transition in α-U. We also show that the phase transition between the α and α_1 structures is accompanied by a strong variation of the longitudinal acoustic branch resulting in a strong decrease of the C_{11} modulus and the bulk modulus.

Higher temperature phases of the actinides could be explored in the future, in particular the ϵ bcc phase of plutonium unstabilized by only taking into account the electronic correlations and hopefully stabilized by the phonon entropy [10].

ACKNOWLEDGMENTS

The authors thank G. H. Lander for comments and suggestions which improved the paper.

[1] J. M. Wills and O. Eriksson, Phys. Rev. B **45**, 13879 (1992).
[2] L. Fast, O. Eriksson, B. Johansson, J. M. Wills, G. Straub, H. Roeder, and L. Nordström, Phys. Rev. Lett. **81**, 2978 (1998).
[3] N. Richard, S. Bernard, F. Jollet, and M. Torrent, Phys. Rev. B **66**, 235112 (2002).
[4] P. Söderlind, Phys. Rev. B **66**, 085113 (2002).
[5] J. Bouchet, R. C. Albers, M. D. Jones, and G. Jomard, Phys. Rev. Lett. **92**, 095503 (2004).
[6] R. C. Albers, Nature (London) **410**, 759 (2001).
[7] S. Baroni, S. de Gironcoli, and A. D. Corso, Rev. Mod. Phys. **73**, 515 (2001).
[8] J. Bouchet, F. Jollet, and G. Zerah, Phys. Rev. B **74**, 134304 (2006).
[9] P. Söderlind, B. Grabowski, L. Yang, A. Landa, T. Björkman, P. Souvatzis, and O. Eriksson, Phys. Rev. B **85**, 060301 (2012).
[10] X. Dai, S. Savrasov, G. Kotliar, A. Migliori, H. Ledbetter, and E. Abrahams, Science **300**, 953 (2003).
[11] G. H. Lander, E. S. Fisher, and S. D. Bader, Adv. Phys. **43**, 1 (1994).
[12] W. P. Crummett, H. G. Smith, R. M. Nicklow, and N. Wakabayashi, Phys. Rev. B **19**, 6028 (1979).
[13] H. G. Smith, N. Wakabayashi, W. P. Crummett, R. M. Nicklow, G. H. Lander, and E. S. Fisher, Phys. Rev. Lett. **44**, 1612 (1980).
[14] J. Bouchet, Phys. Rev. B **77**, 024113 (2008).
[15] S. Raymond, J. Bouchet, G. H. Lander, M. Le Tacon, G. Garbarino, M. Hoesch, J.-P. Rueff, M. Krisch, J. C. Lashley, R. K. Schulze, and R. C. Albers, Phys. Rev. Lett. **107**, 136401 (2011).
[16] A. Dewaele, J. Bouchet, F. Occelli, M. Hanfland, and G. Garbarino, Phys. Rev. B **88**, 134202 (2013).
[17] P. Souvatzis, O. Eriksson, M. I. Katsnelson, and S. P. Rudin, Phys. Rev. Lett. **100**, 095901 (2008).
[18] O. Hellman, I. A. Abrikosov, and S. I. Simak, Phys. Rev. B **84**, 180301 (2011).
[19] O. Hellman, P. Steneteg, I. A. Abrikosov, and S. I. Simak, Phys. Rev. B **87**, 104111 (2013).
[20] The ABINIT code is a common project of the Catholic University of Louvain (Belgium), Corning Incorporated, CEA (France), and other collaborators (URL http://www.abinit.org).
[21] X. Gonze, B. Amadon, P.-M. Anglade, J.-M. Beuken, F. Bottin, P. Boulanger, F. Bruneval, D. Caliste, R. Caracas, M. Côté, T. Deutsch, L. Genovese, P. Ghosez, M. Giantomassi, S. Goedecker, D. Hamann, P. Hermet, F. Jollet, G. Jomard, S. Leroux, M. Mancini, S. Mazevet, M. Oliveira, G. Onida, Y. Pouillon, T. Rangel, G.-M. Rignanese, D. Sangalli, R. Shaltaf, M. Torrent, M. Verstraete, G. Zerah, and J. Zwanziger, Comput. Phys. Commun. **180**, 2582 (2009).
[22] P. E. Blöchl, Phys. Rev. B **50**, 17953 (1994).

[23] M. Torrent, F. Jollet, F. Bottin, G. Zerah, and X. Gonze, Comput. Mater. Sci. **42**, 337 (2008).
[24] J. P. Perdew, K. Burke, and M. Ernzerhof, Phys. Rev. Lett. **77**, 3865 (1996).
[25] A. N. Chantis, R. C. Albers, M. D. Jones, M. van Schilfgaarde, and T. Kotani, Phys. Rev. B **78**, 081101 (2008).
[26] J.-W. Yang, T. Gao, B.-Q. Liu, G.-A. Sun, and B. Chen, Phys. Status Solidi B **252**, 521 (2015).
[27] P. Söderlind, B. Sadigh, V. Lordi, A. Landa, and P. Turchi, J. Nucl. Mater. **444**, 356 (2014).
[28] N. Holzwarth, A. Tackett, and G. Matthews, Comput. Phys. Commun. **135**, 329 (2001).
[29] ATOMPAW is a general license public code developed at Wake Forest University. Some of its capabilities have been developed at the Commissariat à l'énergie atomique (http://pwpaw.wfu.edu).
[30] A. Dewaele, M. Torrent, P. Loubeyre, and M. Mezouar, Phys. Rev. B **78**, 104102 (2008).
[31] L. T. Llyod, J. Nucl. Mater. **3**, 67 (1961).
[32] L. T. Llyod and C. S. Barrett, J. Nucl. Mater. **18**, 55 (1966).
[33] C. S. Barrett, M. H. Mueller, and R. L. Hitterman, Phys. Rev. **129**, 625 (1963).
[34] T. Le Bihan, S. Heathman, M. Idiri, G. H. Lander, J. M. Wills, A. C. Lawson, and A. Lindbaum, Phys. Rev. B **67**, 134102 (2003).
[35] F. Bottin, S. Leroux, A. Knyazev, and G. Zérah, Comput. Mater. Sci. **42**, 329 (2008).
[36] R. Powell and Y. Touloukian, Science **181**, 999 (1973).
[37] E. J. Nelson, P. G. Allen, K. J. M. Blobaum, M. A. Wall, and C. H. Booth, Phys. Rev. B **71**, 184113 (2005).
[38] J. C. Marmeggi, G. H. Lander, S. van Smaalen, T. Brückel, and C. M. E. Zeyen, Phys. Rev. B **42**, 9365 (1990).
[39] R. Springell, R. C. C. Ward, J. Bouchet, J. Chivall, D. Wermeille, P. S. Normile, S. Langridge, S. W. Zochowski, and G. H. Lander, Phys. Rev. B **89**, 245101 (2014).
[40] J. Marmeggi, R. Currat, A. Bouvet, and G. Lander, Physica B **276**, 272 (2000).
[41] E. S. Fisher and H. J. McSkimin, J. Appl. Phys. **29**, 1473 (1958).
[42] E. S. Fisher, J. Nucl. Mater. **18**, 39 (1966).
[43] E. S. Fisher and D. Dever, Phys. Rev. **170**, 607 (1968).
[44] E. S. Fisher and H. J. McSkimmin, Phys. Rev. **124**, 67 (1961).
[45] G. Simmons and H. Wang, *Single Crystal Elastic Constants and Calculated Aggregate Properties: A Handbook* (MIT Press, Cambridge, MA, 1971).